Evaluation of Ganglion Cell–Inner Plexiform Layer Thinning in Eyes With Optic Disc Hemorrhage: A Trend-Based Progression Analysis

Won June Lee,[1,2] Young Kook Kim,[1,2] Ki Ho Park,[1,2] and Jin Wook Jeoung[1,2]

[1]Department of Ophthalmology, Seoul National University College of Medicine, Seoul, Korea
[2]Department of Ophthalmology, Seoul National University Hospital, Seoul, Korea

Correspondence: Jin Wook Jeoung, Department of Ophthalmology, Seoul National University Hospital, Seoul National University College of Medicine, 101 Daehak-ro, Jongno-gu, Seoul 03080, Korea; neuroprotect@gmail.com.

Submitted: July 4, 2017
Accepted: November 20, 2017

Citation: Lee WJ, Kim YK, Park KH, Jeoung JW. Evaluation of ganglion cell–inner plexiform layer thinning in eyes with optic disc hemorrhage: a trend-based progression analysis. *Invest Ophthalmol Vis Sci*. 2017;58:6449–6456. DOI:10.1167/iovs.17-22547

Purpose. To evaluate the rate of change in ganglion cell-inner plexiform layer (GCIPL) thickness measured by optical coherence tomography (OCT) using a trend-based approach in early-stage glaucomatous eyes with disc hemorrhage (DH) and to compare the GCIPL thinning rate with that in glaucomatous eyes without DH.

Methods. This prospective observational study included 46 patients with early-stage open-angle glaucoma and DH who underwent serial spectral-domain OCT measurements for at least 30 months. The GCIPL thinning rate was determined in the global, superior, or inferior hemiretinas and in six macular sectors by linear regression and was compared between glaucomatous eyes with DH and fellow glaucomatous eyes without DH and between glaucomatous eyes with DH and non-DH glaucomatous control eyes.

Results. The GCIPL thinning rate (mean ± standard deviation) was significantly more rapid in glaucomatous eyes with DH than in fellow eyes without DH in the inferior hemiretina (−1.07 ± 0.75 vs. −0.44 ± 0.54 μm/y, $P = 0.001$), inferotemporal sector (−1.13 ± 1.00 vs. −0.61 ± 0.66 μm/y, $P = 0.028$), and inferior sector (−1.33 ± 0.79 vs. −0.42 ± 0.78 μm/y, $P < 0.001$). The GCIPL thinning rate was significantly more rapid in glaucomatous eyes with DH than in glaucomatous controls without DH in the global area (−0.78 ± 0.85 vs. −0.32 ± 0.48 μm/y, $P = 0.002$), the inferior hemiretina (−1.00 ± 0.94 vs. −0.37 ± 0.67 μm/y, $P < 0.001$), and the inferotemporal sector (−1.31 ± 1.07 vs. −0.34 ± 0.75 μm/y, $P < 0.001$).

Conclusions. The GCIPL thinning rate on OCT was significantly more rapid in glaucomatous eyes with DH than in fellow glaucomatous eyes without DH or glaucomatous control eyes without DH. DH could be associated with progression of glaucoma in terms of GCIPL thinning.

Keywords: disc hemorrhage, ganglion cell-inner plexiform layer, optical coherence tomography, glaucoma, trend-based analysis

Disc hemorrhage (DH) is considered to be an important sign of structural glaucomatous damage and has been identified as an important risk factor for progression of glaucoma in numerous studies.[1–5] Our group has previously reported that DH could be a strong risk factor for progression, particularly in the early stage of open-angle glaucoma (OAG) and normal tension glaucoma, along with inadequate reduction in intraocular pressure.[6,7]

However, to date, progression of glaucoma has been evaluated by conventional visual field (VF) testing or by deepening or widening of a circumpapillary retinal nerve fiber layer (cpRNFL) defect using conventional red-free photography or optical coherence tomography (OCT).[1,2,5,8–13] Therefore, in the past, it was only possible to evaluate the relationship between DH and progression of glaucoma using VF or cpRNFL parameters. Currently, the macular inner retinal structures, including parameters related to the ganglion cell-inner plexiform layer (GCIPL), can be used to evaluate the status of glaucoma in the clinical setting. Furthermore, many studies have shown the performance of GCIPL parameters to be comparable with or better than that of cpRNFL parameters in the diagnosis of glaucoma.[14–17] One group reported that eyes with DH showed more rapid retinal ganglion cell (RGC) loss than eyes without DH on the basis of global RGC counts estimated using a model developed by Medeiros and colleagues[18,19] from standard automated perimetry (SAP) and OCT. However, there are still no reports of GCIPL parameters being used to monitor progression of glaucoma or to evaluate the relationship between DH and progression of GCIPL.

The purpose of this study was to evaluate the longitudinal rate of change in GCIPL thickness, as measured by spectral-domain (SD) OCT, in early-stage glaucomatous eyes with DH. Using trend-based analysis, we evaluated the GCIPL thinning rate according to the presence of DH and/or its topographic characteristics.

Methods

The study protocol was approved by the Institutional Review Board of Seoul National University Hospital and followed the tenets of the Declaration of Helsinki for biomedical research. All patients provided informed consent.

Subjects

This study included 46 patients with early-stage OAG and DH who underwent serial SD-OCT measurements for more than 30 months. All the subjects were already enrolled in the ongoing prospective Macular Ganglion Cell Imaging Study that was started in 2011. Patients who had undergone at least four serial GCIPL OCT measurements were considered suitable for inclusion in linear regression analysis and were consecutively enrolled.

All subjects underwent a complete ophthalmologic examination, including visual acuity tests, assessment of manifest refraction, slit-lamp examination, intraocular pressure measurements using Goldmann applanation tonometry, gonioscopy, dilated fundus examination, color disc photography and red-free RNFL photography (TRC-50IX; Topcon Corporation, Tokyo, Japan), Swedish interactive thresholding algorithm (SITA) 30-2 perimetry (Humphrey Field Analyzer II; Carl Zeiss Meditec, Jena, Germany), and Cirrus HD-OCT 4000 (Carl Zeiss Meditec, Inc., Dublin, CA, USA). Both eyes were imaged with the Cirrus HD-OCT and examined by SAP every 6–12 months for at least 30 months.

The inclusion criteria were as follows: bilateral OAG, clearly visible DH on disc and red-free fundus photographs in either eye at the time of enrollment, both eyes with a mean deviation (MD) of at least −6 dB on VF testing, age 20–79 years, best-corrected visual acuity $\geq$20/40, a spherical equivalent refractive error within $\pm$6.00 diopters, and astigmatism of $\pm$3.00 diopters. The exclusion criteria were as follows: a history of ophthalmic surgery (such as glaucoma-filtering surgery), any other ocular disease that could interfere with visual function, any media opacity that would significantly interfere with acquisition of OCT images, and inability to obtain high-quality OCT image (i.e., if all images had a signal strength <6).

Patients with OAG were identified by the presence of glaucomatous optic disc changes with corresponding glaucomatous VF defects and an open angle confirmed by gonioscopic examination. Glaucomatous optic disc changes were defined as neuroretinal rim thinning, notching, excavation, or RNFL defects. Glaucomatous VF defects were defined as follows: (1) glaucoma hemifield test values outside the normal limits; (2) three or more abnormal points with a less than 5% probability of being normal and of which at least one point had a pattern deviation probability of less than 1%; or (3) a pattern standard deviation (PSD) probability of less than 5%. The VF defects were confirmed on two consecutive reliable tests (fixation loss rate $\leq$20%, false-positive and false-negative error rates $\leq$25%).

If a patient had bilateral DH, one eye was randomly chosen as the study eye prior to analysis. Patients who had OAG without DH at baseline and during follow-up were enrolled in the control group. When both eyes met all eligibility criteria for inclusion in the control group, one eye was randomly chosen as a control prior to analysis.

Characteristics of DH

DH was defined as an isolated hemorrhage observed either on the optic disc or in the peripapillary retina and extending to the disc rim. Two observers (WJL, JWJ) measured the topographic patterns and recurrence of DH using digital color stereo disc photographs and red-free RNFL photographs. The method has been described in detail elsewhere.[20,21]

The proximal location (cup wall, cup margin, disc rim, or disc margin), angular extent (circumferential angle formed by two lines drawn from the disc center to the two points farthest from each other circumferentially), corrected area (calculated in consideration of the magnification factors related to the SD-OCT camera and the eye by substituting the subject's axial length), and corrected length of maximum radial extent of DH (the straight distance from the center of the optic disc to the point of maximum radial extent of DH, which compensates for the magnification factor) were assessed to determine the topographic characteristics of DH. Nonrecurrent DH was defined as DH detected only once during follow-up. Recurrent DH was defined when any new DH, regardless of the location, was detected during follow-up. The number of DH recurrences detected during follow-up was recorded, and the characteristics of these recurrences, including the location of recurrent DH in relation to the initial DH, were evaluated.

OCT Imaging

A Cirrus HD-OCT 4000 machine was used to obtain the OCT images. The optic disc cube scan and ganglion cell analysis (GCA) protocol for macular cube scanning (macular cube, 6×6 mm^2, 200×200 pixels) were used for diagnosis and follow-up of glaucoma in the clinic.

The optic disc cube scan imaged the optic disc region in an area of 6×6 mm^2 (200×200 pixels). The RNFL thickness was measured in each pixel, and an RNFL thickness map was generated. A cpRNFL circle measuring 3.46 mm in diameter and consisting of 256 A-scans was then automatically positioned around the optic disc.

The macular cube scan generated four sets of 128 horizontal B-scans, each comprising 512 A-scans, centered on the 6×6 mm^2 macular region. The built-in GCA algorithm (Cirrus HD-OCT software, version 10.0) detected and measured macular GCIPL thickness within a $6 \times 6 \times 2$-mm cube in an elliptical annulus around the fovea. The GCA algorithm identified the outer boundary of the RNFL as well as the outer boundary of the inner plexiform layer. The difference between the RNFL and inner plexiform layer outer boundary segmentation yielded the combined thickness of the GCIPL. All OCT images located a centered optic disc or fovea were well focused and had a signal strength $\geq$6.

Calculation of Cirrus HD-OCT GCIPL and cpRNFL Thinning Rates and VF Indices Changing Rates

Linear regression analysis versus time was performed for GCIPL thickness in the global, superior, inferior hemiretina, and six sectors (superior, superotemporal, superonasal, inferior, inferotemporal, and inferonasal) for each eye of each subject in order to determine the rate of change in GCIPL thickness (expressed in micrometers per year), as described previously.[22] The rate of change in RNFL thickness was calculated in the same manner as that used in the global, superior, and inferior regions. Images with a signal strength of <6, images that were out of focus in reference to the fovea or optic disc, and cases of algorithm segmentation failure were excluded from the linear regression analysis.

The rate of change in VF parameters was calculated in the same manner as that used for the MD, PSD, and VF index (VFI). Unreliable VF results were excluded from linear regression analysis.

Determination of Glaucoma Progression

Color disc photographs, red-free RNFL photographs, and VF tests were performed and assessed according to the routine follow-up schedule. The patient's structural progression status was determined by structural changes on disc and RNFL photography, as described previously.[6] Progressive optic disc changes (i.e., focal or diffuse narrowing, neuroretinal rim notching, increased cup-to-disc ratio, adjacent vasculature

position shift) were identified by comparing serial photographic disc images and regarded as progression of glaucoma. Changes in an RNFL defect were determined using serial RNFL photographs and defined as the appearance of a new defect or an increase in width or depth of an existing defect. These changes were considered to indicate structural progression.[23] Two observers (WJL, JWJ) masked to all other patient information independently evaluated all photographs. In cases of disagreement in structural progression, a third glaucoma specialist (KHP) served as an adjudicator.

Functional progression was determined by event analysis using the commercial guided progression analysis (GPA) software provided by the VF device. Functional progression was confirmed when at least three test points were flagged as having deteriorated significantly at the same test point locations in three consecutive fields (the software classifies VF progression as "likely progression").[4,24] These changes also had to have been observed at the final visit.

Statistical Analyses

All statistical tests were performed using statistics software (PASW Statistics version 18; SPSS, Inc., Chicago, IL, USA) and MedCalc (MedCalc Software, Ostend, Belgium). The paired *t*-test was used to compare the GCIPL thinning rate between glaucomatous eyes with DH and fellow eyes without DH. The independent *t*-test was used to compare the GCIPL thinning rate between glaucomatous eyes with DH and glaucomatous controls without DH. Pearson correlation for continuous variables, the independent *t*-test for binary categorical variables, and 1-way analysis of variance for multiple categorical variables were used to evaluate the association between GCIPL thinning rate obtained from linear regression and the characteristics of DH. P values < 0.05 were considered to be statistically significant. The study data are shown as the mean $\pm$ standard deviation.

Results

The study included 46 eyes of 46 patients with early-stage OAG and DH who fulfilled the inclusion criteria. Of these, 32 patients had DH in one eye and 14 had DH in both eyes. Forty-nine non-DH eyes of 49 patients with early-stage OAG were enrolled as the control group without DH.

Clinical Demographics

The clinical demographic characteristics of the patients at baseline are shown in Table 1. Most of the DHs were located in the inferior portion (41 eyes, 89.1%). The mean number of DH recurrences was 1.76 $\pm$ 0.90, and recurrent DHs were observed in 23 eyes (50.0%). Other topographic features of the DHs are described in Table 1.

Comparison of Ocular Characteristics Between Eyes With DH and Contralateral Eyes Without DH

A comparison of the ocular characteristics of the eyes with DH and fellow eyes without DH is provided in Supplementary Table S1. There were no significant differences between the two groups of eyes, except for baseline IOP.

Comparison of Ocular Characteristics Between Eyes With DH and Control Eyes Without DH

A comparison of the ocular characteristics of the eyes with DH and control eyes without DH is provided in Supplementary Table S2. There were no significant differences between the two groups of eyes, except for sex and the GCIPL thickness of the inferotemporal sector at baseline.

Comparison of GCIPL and RNFL Thinning Rate and VF Parameters Changing Rate Between Groups

A comparison of the GCIPL and RNFL thinning rate in eyes with DH and fellow eyes without DH is provided in Table 2. In the eyes with DH, the GCIPL thinning rate in the inferior hemiretina, inferotemporal sector, inferior sector, and inferonasal sector was significantly more rapid than that in the fellow eyes without DH (–1.07 $\pm$ 0.75 vs. –0.44 $\pm$ 0.54 μm/y, $P = 0.001$; –1.13 $\pm$ 1.00 vs. –0.61 $\pm$ 0.66 μm/y, $P = 0.020$; –1.30 $\pm$ 0.79 vs. –0.42 $\pm$ 0.78 μm/y, $P < 0.001$; and –0.78 $\pm$ 1.16 vs. –0.29 $\pm$ 0.69 μm/y, $P = 0.039$, respectively). A representative case of a patient with glaucoma and DH and trend-based analysis of the GCIPL thinning rate is shown in Figure 1. The RNFL thinning rate in the inferior portion was significantly more rapid in the eyes with DH than in the fellow eyes without DH (–1.87 $\pm$ 1.91 vs. –0.85 $\pm$ 1.95 μm/y, $P = 0.033$). The rate of change in VF parameters was not significantly different between the groups.

A comparison of the GCIPL thinning rate in eyes with DH and control eyes without DH is provided in Table 3. The GCIPL thinning rate in the global, inferior hemiretina, inferotemporal, and inferior sectors in the eyes with DH was significantly more rapid than that in the control eyes without DH (–0.78 $\pm$ 0.85 vs. –0.32 $\pm$ 0.48 μm/y, $P = 0.002$; –1.00 $\pm$ 0.94 vs. –0.37 $\pm$ 0.67 μm/y, $P < 0.001$; –1.31 $\pm$ 1.07 vs. –0.34 $\pm$ 0.75 μm/y, $P < 0.001$; and –1.29 $\pm$ 0.95 vs. –0.43 $\pm$ 0.99 μm/y, $P < 0.001$, respectively). The RNFL thinning rate in the inferior portion was significantly more rapid in the eyes with DH than that in the control eyes without DH (–2.18 $\pm$ 1.99 vs. –1.28 $\pm$ 1.38 μm/y, $P = 0.012$). The rate of change in VF parameters was not significantly different between the groups.

A comparison of the GCIPL thinning rate between the groups is shown in Figure 2. The GCIPL thinning rate in the global average area was significantly more rapid in the eyes with DH than in the control eyes without DH (Fig. 2A). The GCIPL thinning rate was significantly more rapid in the inferior hemiretina in eyes with DH than the rates in fellow eyes and control eyes without DH (Fig. 2B). In the inferotemporal area, eyes with DH showed significantly more rapid GCIPL thinning than the fellow eyes and control eyes without DH.

Association of Rate of GCIPL Thinning With Recurrence and Topographic Characteristics of DH

There was no significant association between GCIPL thinning rate and recurrence of DH, recurrent DH at 1 clock hour (30 degree) of initial DH location, or recurrent DH at the same location (Table 4). The association between the topographic characteristics of the DH and the GCIPL thinning rate was analyzed and is summarized in Supplementary Tables S3 and S4. There were no significant association between GCIPL thinning rate and the topographic characteristics of the DH, including angular extent, corrected length of maximum radial extent, number, and proximal location. Only the corrected DH areas were significantly correlated with the rate of GCIPL thinning of the global average and inferotemporal sectors ($r = 0.366$, $P = 0.015$ and $r = 0.298$, $P = 0.049$, respectively). The rates of GCIPL and RNFL thinning of the affected hemiretina (corresponding to the DH location) were significantly more rapid than those of the unaffected hemiretina (–1.06 $\pm$ 0.94 vs. –0.39 $\pm$ 0.97 μm/y, $P < 0.001$, and –2.21 $\pm$ 1.93 vs. –1.32 $\pm$ 1.55 μm/y, $P = 0.004$, respectively; Supplementary Table S5).

Investigative Ophthalmology & Visual Science

Table 1. Clinical Characteristics and Demographics of Eyes With DH

	Patients With DH, $n = 46$
Bilateral DH	14 patients
Location of DH	
Superior portion	5 (10.9%)
Inferior portion	41 (89.1%)
Proximal location of DH	
Cup wall	2 (4.3%)
Cup margin	14 (30.4%)
Disc rim	17 (37.0%)
Disc margin	13 (28.3%)
Angular extent of DH, deg	22.1 ± 14.4
Corrected DH area, mm^2	0.090 ± 0.153
Corrected LMRE of DH, mm	1.24 ± 0.28
Number of DH recurrences	1.76 ± 0.90
1 time (no recurrence)	23 (50.0%)
2 times	13 (28.3%)
3 times	8 (17.4%)
Over 4 times	2 (4.3%)
Recurrent DH	23 eyes (50.0%)
Recurrent at 1 clock hour	14 (60.9%)
Recurrent at more than 1 clock hour	9 (39.1%)
Recurrent at same location	7 (30.4%)
Recurrent at different locations	16 (69.6%)

The data are shown as the mean and standard deviation unless otherwise indicated. LMRE, length of maximum radial extent.

Discussion

OCT parameters are widely used in trials currently to analyze progression of glaucoma. Event-based analysis of OCT GPA focuses on newly developed damage, which evaluates the difference in RNFL thickness between baseline and follow-up examination from the OCT RNFL thickness map.[25] When the differences exceed the test-retest variability, the pixels or parameters are regarded as showing significant changes.

Our group recently performed a study that evaluated the GCIPL thinning rate using a trend-based approach in glaucomatous eyes with a localized RNFL defect and assessed the ability of the GCIPL thinning rate to predict progression of glaucoma.[22] We found that the GCIPL thinning rate was more rapid in eyes that progressed than in eyes that did not progress and that analysis of the GCIPL thinning rate is useful for discriminating the progression of glaucoma.[22] Recently, GPA has been developed for the macular GCIPL protocol and introduced with commercially available software.[24] On this background, we hypothesized that DH, a well-known factor in progression of glaucoma, could affect the GCIPL thinning rate, and performed the present study to test this hypothesis.

Recently, Gracitelli et al.[18] reported that eyes with DH showed faster rates of RGC loss than eyes without DH. Because functional status ultimately reflects dysfunction or loss of RGC, evaluating RGC could be essential when determining the status and progression of glaucoma. Medeiros et al.[19] developed an empirical formula for estimation of RGC counts using a combination of OCT images of the RNFL and SAP sensitivity values and estimated longitudinal rates of RGC loss. The results of our study are consistent with those of the previous studies. However, we believe that our present study has some additional strengths. First, we used a more convenient commercially available method, that is, the GCA software in the Cirrus OCT. Second, we examined rates of GCIPL loss in specific areas (i.e., global average, both hemiretinas, and six sectors in the macular area) that were not evaluated in the previous reports.

In our analysis, the GCIPL thinning rate in the inferior area, including the inferior hemiretina and inferotemporal sectors, was more rapid than in the other sectors, and there was a

Table 2. Comparison of Rates of GCIPL Change Between Eyes With DH and Contralateral Eyes Without DH

	Eyes With DH, $n = 32$	Contralateral Eye, $n = 32$	*P* Value
Rate of GCIPL thickness change, μm/y			
Average	−0.79 ± 0.80	−0.57 ± 0.90	0.150*
Superior hemiretina	−0.49 ± 1.10	−0.69 ± 1.57	0.268*
Inferior hemiretina	−1.07 ± 0.75	−0.44 ± 0.54	**0.001***
Superonasal sector	−0.32 ± 0.98	−0.51 ± 1.25	0.345*
Superior sector	−0.60 ± 2.01	−0.83 ± 2.71	0.230*
Superotemporal sector	−0.53 ± 0.90	−0.72 ± 0.95	0.365*
Inferotemporal sector	−1.13 ± 1.00	−0.61 ± 0.66	**0.020***
Inferior sector	−1.30 ± 0.79	−0.42 ± 0.78	**<0.001***
Inferonasal sector	−0.78 ± 1.16	−0.29 ± 0.69	**0.039***
Rate of RNFL thickness change, μm/y			
Average	−1.10 ± 1.08	−0.71 ± 0.82	0.127*
Superior	−1.21 ± 1.46	−1.40 ± 1.81	0.685*
Inferior	−1.87 ± 1.91	−0.85 ± 1.95	**0.033***
Rate of VF change			
MD (dB/y)	−0.10 ± 0.58	−0.00 ± 0.53	0.349*
PSD (dB/y)	0.11 ± 0.65	−0.03 ± 0.33	0.241*
VFI (%/y)	−0.70 ± 1.48	−0.34 ± 1.21	0.277*
Total progression of glaucoma, no. (%)†	13 (40.6)	8 (25.0)	0.183‡
Structural progression, no. (%)§	12 (37.5)	5 (15.6)	**0.048‡**
Functional progression, no. (%)‖	4 (12.5)	4 (12.5)	1.000‡

The data are shown as the mean and standard deviation unless otherwise indicated. Bold values indicates statistically significant with *P* Value ≤ 0.05.

* Paired *t*-test.

† Combined structural and/or functional progression.

‡ χ^2 test.

§ Determined by disc and RNFL photography.

‖ Determined by GPA of Humphrey VF.

Investigative Ophthalmology & Visual Science

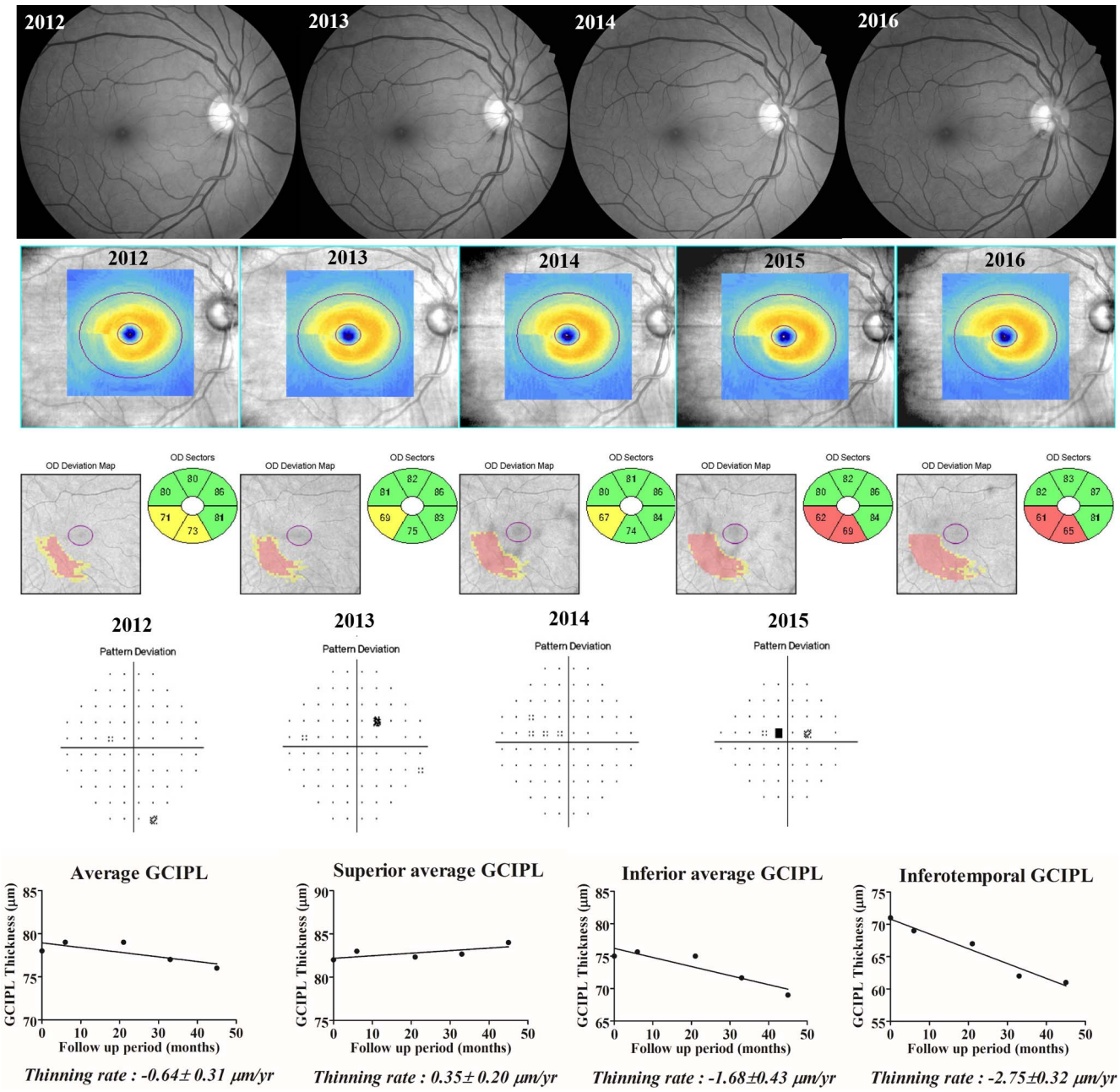

FIGURE 1. A representative case of a patient with glaucoma and DH. Recurrent DH developed at the 7 o'clock location in 2012, 2013, and 2016. The localized RNFL defect in the inferotemporal region widened and deepened with the passage of time. Thinning of the GCIPL at the inferior hemiretina progressed, especially at the inferotemporal sector. The GCIPL thinning rate calculated with linear regression was significantly more rapid at the inferior hemiretina than at the superior hemiretina.

significant difference between eyes with and without DH, whether fellow eyes or control eyes were used for comparison. The high GCIPL thinning rate in the inferior area would be attributable to the high prevalence of inferiorly located (especially inferotemporal) DH in our study population. This finding is in agreement with a previous report that localized thinning of the RNFL and progression of glaucoma were spatially compatible with the location of DH and that the RNFL thinning rate was most rapid in the inferotemporal area (especially at the 7 o'clock position).[12] It is also in accordance with many other studies showing that DHs occur most frequently in the inferotemporal area.[1,20,26–28] Recently, Hood[29] proposed that early glaucomatous damage involves the macula and is often associated with localized RNFL thinning in a narrow region of the disc known as the macular vulnerability zone. In our study, we showed that location of progression in the macula corresponds to the macular vulnerability zone in which DH frequently occurred.

The clinical significance of recurrent DH remains controversial. Some studies have reported more pronounced progressive changes at the optic disc in eyes with recurrent DH than in eyes without recurrent DH.[1,13] However, the present study demonstrated that recurrence of DH was not associated with the GCIPL thinning rate as part of structural progression. Our results are partially consistent with other studies showing that recurrent DH is not in itself associated with greater

Table 3. Comparison of Mean Values of the Rates of GCIPL Thickness Change Between Eyes With DH and Eyes Without DH (Controls)

	Eyes With DH, $n = 46$	Non-DH Eye, $n = 49$	*P* Value
Rate of GCIPL thickness change, μm/y			
Average	−0.78 ± 0.85	−0.32 ± 0.48	**0.002***
Superior hemiretina	−0.44 ± 1.00	−0.32 ± 0.55	0.472*
Inferior hemiretina	−1.00 ± 0.94	−0.37 ± 0.67	**<0.001***
Superonasal sector	−0.25 ± 1.25	−0.23 ± 0.65	0.919*
Superior sector	−0.55 ± 1.70	−0.40 ± 0.70	0.590*
Superotemporal sector	−0.51 ± 0.82	−0.36 ± 0.75	0.351*
Inferotemporal sector	−1.31 ± 1.07	−0.34 ± 0.75	**<0.001***
Inferior sector	−1.29 ± 0.95	−0.43 ± 0.99	**<0.001***
Inferonasal sector	−0.42 ± 2.14	−0.34 ± 0.75	0.824*
Rate of RNFL thickness change, μm/y			
Average	−1.18 ± 1.06	−0.86 ± 0.96	0.127*
Superior	−1.35 ± 1.49	−1.52 ± 1.85	0.644*
Inferior	−2.18 ± 1.99	−1.28 ± 1.38	**0.012***
Rate of VF change			
MD, dB/y	−0.19 ± 0.67	−0.05 ± 0.66	0.309*
PSD, dB/y	0.12 ± 0.58	0.11 ± 0.75	0.918*
VFI, %/y	−0.86 ± 1.89	−0.43 ± 1.36	0.214*
Total progression of glaucoma, no. (%)†	24 (52.2)	13 (26.5)	**0.010‡**
Structural progression§	23 (50.0)	9 (18.4)	**0.001‡**
Functional progression‖	9 (19.6)	7 (14.3)	0.492‡

The data are shown as the mean and standard deviation unless otherwise indicated. Bold values indicates statistically significant with *P* Value ≤ 0.05.

* Independent *t*-test.

† Combined structural and/or functional progression.

‡ χ^2 test.

§ Determined by disc and RNFL photography.

‖ Determined by GPA of Humphrey VF.

progression of glaucoma.[21,30] Eyes with recurrent DH may have received intensified treatment and may have been followed up more closely. Intensifying treatment can slow the rate of RNFL thinning in eyes with DH and should be considered when interpreting the clinical significance of recurrent DH.[31]

The present study has some limitations. First, the number of GCIPL image acquisitions was limited. The mean number of GCIPL acquisitions in the eyes with DH was only 5.1 ± 0.8 (range, 4–7) and the mean duration of follow-up of the GCIPL using OCT was only 51.1 ± 10.8 (range, 31–80) months. Future studies with large sample sizes and longer follow-up durations will be needed to further elucidate the relationship between the topographic characteristics of DHs and GCIPL thinning rates. Second, a causal relationship between DH and the GCIPL progression could not be established. It remains unclear whether DH is a cause or a result of GCIPL progression. If DH is a result of progression of the disease, it would be more common in eyes that are susceptible to progression. Third, patients with early-stage OAG were assessed in this study. However, DH can be detected in any

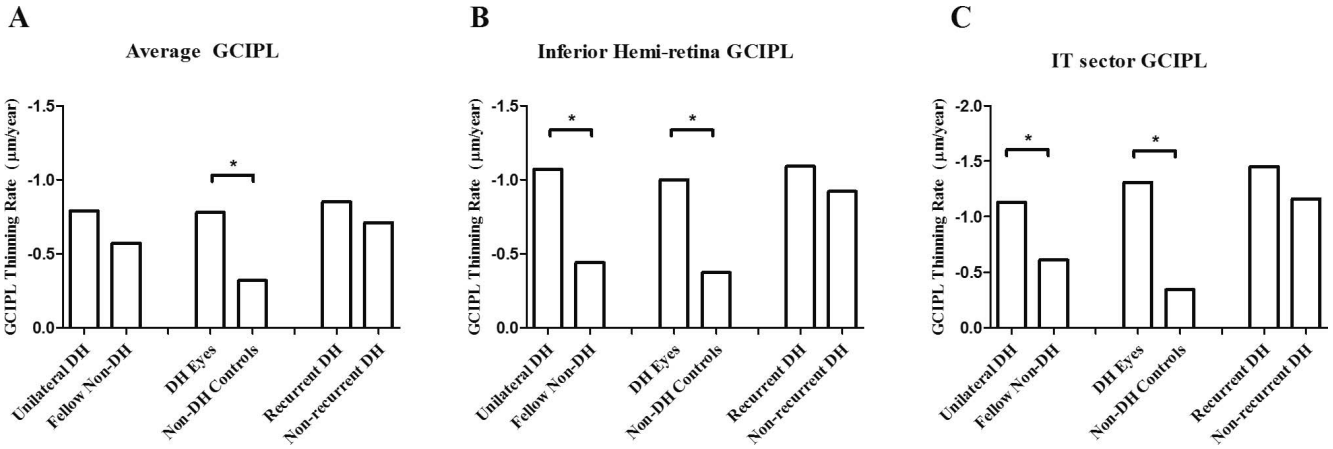

Figure 2. The GCIPL thinning rate is shown in each group. The average GCIPL thinning rate was more rapid in eyes with DH than in controls without DH. There were no differences in terms of the average GCIPL thinning rate between the other groups (**A**). The eyes with DH showed more rapid GCIPL thinning in the inferior hemiretina and the inferotemporal sector than fellow eyes or control eyes without DH (**B**, **C**). There were no differences in terms of GCIPL thinning rate in the global average, inferior hemiretina, or inferotemporal sector between the group with recurrent DH and the group without recurrent DH (**A**–**C**). *$P < 0.05$.

Table 4. Rate of GCIP Changes in Glaucoma Patients With Recurrent DH

GCIPL Thickness Changes, μm/y		Diff.*	95% CI*	*P* Value*
Average GCIPL				
Nonrecurrent DH	Recurrent DH			
−0.71 ± 1.05	−0.85 ± 0.60	0.25	−0.37 to 0.65	0.581
Recurrent DH at 1 clock hour	Recurrent DH at more than 1 clock hour			
−0.71 ± 0.70	−1.06 ± 0.33	0.34	−0.18 to 0.87	0.186
Recurrent DH at same location	Recurrent DH at different location			
−0.60 ± 0.49	−0.96 ± 0.63	0.36	−0.20 to 0.92	0.194
IT sector GCIPL				
Nonrecurrent DH	Recurrent DH			
−1.16 ± 1.01	−1.45 ± 1.13	0.32	−0.34 to 0.93	0.358
Recurrent DH at 1 clock hour	Recurrent DH at more than 1 clock hour			
−1.39 ± 1.31	−1.55 ± 0.84	0.16	−0.86 to 1.19	0.744
Recurrent DH at same location	Recurrent DH at different location			
−1.12 ± 1.14	−1.60 ± 1.14	0.48	−0.59 to 1.55	0.360

The data are shown as the mean and standard deviation unless otherwise indicated.
* Comparison between groups using independent *t*-test. Point estimate of difference, precision estimates (95% confidence interval).

stages of glaucoma.[32,33] Further studies in eyes with various stages of glaucoma are necessary.

In conclusion, trend-based analysis showed that the GCIPL thinned more rapidly in eyes with DH than in eyes without DH, especially in the inferotemporal sector. Our results provide further evidence that DH is an important indicator of progression of glaucoma. Careful observation in specific GCIPL sectors would be helpful when evaluating disease progression in glaucomatous eyes with DH.

Acknowledgments

Disclosure: **W.J. Lee**, None; **Y.K. Kim**, None; **K.H. Park**, None; **J.W. Jeoung**, None

References

1. Kim SH, Park KH. The relationship between recurrent optic disc hemorrhage and glaucoma progression. *Ophthalmology*. 2006;113:598–602.
2. Drance S, Anderson DR, Schulzer M; for Collaborative Normal-Tension Glaucoma Study Group. Risk factors for progression of visual field abnormalities in normal-tension glaucoma. *Am J Ophthalmol*. 2001;131:699–708.
3. Bengtsson B, Leske MC, Yang Z, Heijl A; for the Early Manifest Glaucoma Trial Group. Disc hemorrhages and treatment in the early manifest glaucoma trial. *Ophthalmology*. 2008;115:2044–2048.
4. Leske MC, Heijl A, Hyman L, et al. Predictors of long-term progression in the early manifest glaucoma trial. *Ophthalmology*. 2007;114:1965–1972.
5. Medeiros FA, Alencar LM, Sample PA, Zangwill LM, Susanna R Jr, Weinreb RN. The relationship between intraocular pressure reduction and rates of progressive visual field loss in eyes with optic disc hemorrhage. *Ophthalmology*. 2010;117:2061–2066.
6. Kim KE, Jeoung JW, Kim DM, Ahn SJ, Park KH, Kim SH. Long-term follow-up in preperimetric open-angle glaucoma: progression rates and associated factors. *Am J Ophthalmol*. 2015;159:160–168.
7. Jeong JH, Park KH, Jeoung JW, Kim DM. Preperimetric normal tension glaucoma study: long-term clinical course and effect of therapeutic lowering of intraocular pressure. *Acta Ophthalmol*. 2014;92:e185–193.
8. Lee EJ, Kim TW, Weinreb RN, Park KH, Kim SH, Kim DM. Trend-based analysis of retinal nerve fiber layer thickness measured by optical coherence tomography in eyes with localized nerve fiber layer defects. *Invest Ophthalmol Vis Sci*. 2011;52:1138–1144.
9. Leung CK. Diagnosing glaucoma progression with optical coherence tomography. *Curr Opin Ophthalmol*. 2014;25:104–111.
10. Leung CK, Cheung CY, Weinreb RN, et al. Evaluation of retinal nerve fiber layer progression in glaucoma: a study on optical coherence tomography guided progression analysis. *Invest Ophthalmol Vis Sci*. 2010;51:217–222.
11. Wollstein G, Schuman JS, Price LL, et al. Optical coherence tomography longitudinal evaluation of retinal nerve fiber layer thickness in glaucoma. *Arch Ophthalmol*. 2005;123:464–470.
12. Suh MH, Park KH, Kim H, et al. Glaucoma progression after the first-detected optic disc hemorrhage by optical coherence tomography. *J Glaucoma*. 2012;21:358–366.
13. Hwang YH, Kim YY, Kim HK, Sohn YH. Changes in retinal nerve fiber layer thickness after optic disc hemorrhage in glaucomatous eyes. *J Glaucoma*. 2014;23:547–552.
14. Jeoung JW, Choi YJ, Park KH, Kim DM. Macular ganglion cell imaging study: glaucoma diagnostic accuracy of spectral-domain optical coherence tomography. *Invest Ophthalmol Vis Sci*. 2013;54:4422–4429.
15. Mwanza JC, Durbin MK, Budenz DL, et al. Glaucoma diagnostic accuracy of ganglion cell-inner plexiform layer thickness: comparison with nerve fiber layer and optic nerve head. *Ophthalmology* 2012;119:1151–1158.
16. Jeong JH, Choi YJ, Park KH, Kim DM, Jeoung JW. Macular ganglion cell imaging study: covariate effects on the spectral domain optical coherence tomography for glaucoma diagnosis. *PLoS One*. 2016;11:e0160448.
17. Lee SY, Jeoung JW, Park KH, Kim DM. Macular ganglion cell imaging study: interocular symmetry of ganglion cell-inner plexiform layer thickness in normal healthy eyes. *Am J Ophthalmol*. 2015;159:315–323.
18. Gracitelli CP, Tatham AJ, Zangwill LM, Weinreb RN, Liu T, Medeiros FA. Estimated rates of retinal ganglion cell loss in glaucomatous eyes with and without optic disc hemorrhages. *PLoS One*. 2014;9:e105611.
19. Medeiros FA, Zangwill LM, Anderson DR, et al. Estimating the rate of retinal ganglion cell loss in glaucoma. *Am J Ophthalmol*. 2012;154:814–824.
20. Kim YK, Park KH, Yoo BW, Kim HC. Topographic characteristics of optic disc hemorrhage in primary open-angle glaucoma. *Invest Ophthalmol Vis Sci*. 2014;55:169–176.

21. Park HY, Kim EK, Park CK. Clinical significance of the location of recurrent optic disc hemorrhage in glaucoma. *Invest Ophthalmol Vis Sci*. 2015;56:7524–7534.
22. Lee WJ, Kim YK, Park KH, Jeoung JW. Trend-based analysis of ganglion cell-inner plexiform layer thickness changes on optical coherence tomography in glaucoma progression. *Ophthalmology*. 2017;124:1383–1391.
23. Suh MH, Kim DM, Kim YK, Kim TW, Park KH. Patterns of progression of localized retinal nerve fibre layer defect on red-free fundus photographs in normal-tension glaucoma. *Eye (Lond)*. 2010;24:857–863.
24. Shin JW, Sung KR, Lee GC, Durbin MK, Cheng D. Ganglion cell-inner plexiform layer change detected by optical coherence tomography indicates progression in advanced glaucoma. *Ophthalmology*. 2017;124;1466–1474.
25. Grewal DS, Tanna AP. Diagnosis of glaucoma and detection of glaucoma progression using spectral domain optical coherence tomography. *Curr Opin Ophthalmol*. 2013;24:150–161.
26. Yamamoto T, Iwase A, Kawase K, Sawada A, Ishida K. Optic disc hemorrhages detected in a large-scale eye disease screening project. *J Glaucoma*. 2004;13:356–360.
27. Diehl DL, Quigley HA, Miller NR, Sommer A, Burney EN. Prevalence and significance of optic disc hemorrhage in a longitudinal study of glaucoma. *Arch Ophthalmol*. 1990;108:545–550.
28. Sonnsjo B, Dokmo Y, Krakau T. Disc haemorrhages, precursors of open angle glaucoma. *Prog Retin Eye Res*. 2002;21:35–56.
29. Hood DC. Improving our understanding, and detection, of glaucomatous damage: an approach based upon optical coherence tomography (OCT). *Prog Retin Eye Res*. 2017;57:46–75.
30. Siegner SW, Netland PA. Optic disc hemorrhages and progression of glaucoma. *Ophthalmology*. 1996;103:1014–1024.
31. Akagi T, Zangwill LM, Saunders LJ, et al. Rates of local retinal nerve fiber layer thinning before and after disc hemorrhage in glaucoma. *Ophthalmology*. 2017;124:1403–1411.
32. Jonas JB, Xu L. Optic disk hemorrhages in glaucoma. *Am J Ophthalmol*. 1994;118:1–8.
33. Kim KE, Park KH. Optic disc hemorrhage in glaucoma: pathophysiology and prognostic significance. *Curr Opin Ophthalmol*. 2017;28:105–112.

Investigative Ophthalmology & Visual Science